Resonant-cavity *p-i-n* photodetector utilizing an electron-beam evaporated Si/SiO_2 microcavity

N. E. J. Hunt, E. F. Schubert, and G. J. Zydzik
AT&T Bell Laboratories, Murray Hill, New Jersey 07974

(Received 5 March 1993; accepted for publication 5 May 1993)

A new photodetector configuration consisting of an integrated Si/SiO_2 microcavity on the light-collecting surface of an InGaAs photodetector is proposed and demonstrated. The resulting resonant cavity *p-i-n* (RC-*PIN*) detector exhibits a narrow spectral response of 14 nm width at a wavelength of 1350 nm, while reflecting all other wavelengths from 1100 to 1700 nm. The high degree of tailorability of spectral position, spectral detection width, and numerical aperature of efficient detection, as well as the ease of layer deposition make the RC-*PIN* attractive for use in wavelength de-multiplexing applications.

There is a strong interest in wavelength selective detectors for use in wavelength-division multiplexing applications. By sending separate signals at different wavelengths through an optical fiber, and detecting these wavelengths separately, one can increase the information capacity of a communications system. The light sources could consist of semiconductor lasers, or narrow-spectrum light emitting diodes (LEDs) such a resonant cavity LED (RCLED).[1] The detection system must be able to demultiplex the signal, i.e., detect the different wavelength signals separately. Each detector in the demultiplexing scheme must be able to detect the light from its design wavelength with good efficiency, while being insensitive to all other wavelengths in order to minimize crosstalk between channels.

Recently, resonant cavity enhanced (RCE) photodetectors have been realized by a number of authors.[2–5] These designs place the absorbing region of a photodetector within a Fabry–Perot resonant cavity consisting of epitaxial semiconductor layers. Such devices can exhibit high speed,[5] can have thin absorption regions, and detect light most strongly at the resonant wavelength of the cavity while reflecting nonresonant wavelengths. These devices, however, require the growth of a thick epitaxial distributed Bragg reflector (DBR) semiconductor mirror below and usually above the active region.

In this work, we propose and demonstrate a novel wavelength-selective photodetector which consists of a *p-i-n* semiconductor and an adjacent optical microcavity. The cavity can consist of any transmitting material combinations (e.g., Si and SiO_2), and may be deposited by a number of deposition techniques. We show that only wavelengths resonant with the cavity mode will be detected. This new detector concept, which we refer to as the resonant-cavity *p-i-n* photodetector (RC-*PIN*), has several advantages over the RCE photodetector including greater tailorability of spectral detection and rejection widths, and easier fabrication and layer thickness control. We demonstrate the operation of such a RC-*PIN* in which 52% of the oncoming light is transmitted through the microcavity at the design wavelength of 1350 nm, and >96% of the light at nearby wavelengths is reflected.

The device structure is shown in Fig. 1. The detector is an InGaAs *p-i-n* photodiode grown on InP, with the light being collected through the substrate. Surface collection is also possible with the present RC-*PIN* design. We deposited two DBR mirrors on the device substrate with a half wavelength thickness ($\lambda/2=2310$ nm) SiO_2 layer in the middle, designed for a resonance vacuum wavelength λ_0 of 1350 nm. The first layer is a SiN_x $\lambda/4$ thickness antireflection coating. In our device this becomes the first layer of a DBR mirror, consisting of alternating low and high index of refraction, $\lambda/4$ layers (1155 nm thickness for SiO_2 and 965 nm thickness for Si). The low index ($n=1.46$) SiO_2 layers and high index ($n=3.5$) amorphous silicon layers were deposited by electron beam evaporation, with the device heated to 100 °C by tungsten lamps. The final growth layer consists of *e*-beam evaporated Al_2O_3 in order to tune the reflectivity of the top mirror for maximum transmission at the resonant wavelength of 1350 nm. The cavity will be at resonance, and will transmit light if the following resonance condition is met:

$$\phi_{R1}+\phi_{R2}+\frac{4\pi n_{\min}L_{\text{mid}}}{\lambda_0}=2m\pi, \quad m\in\mathbb{I}. \tag{1}$$

The values ϕ_{R1} and ϕ_{R2} are the reflection phases at the middle layer/DBR interfaces, while n_{mid} is the refractive index of the middle layer. For $\lambda_0=1350$ nm in our device, $\phi_{R1}=\pi$ and $\phi_{R2}=\pi$ and $L_{\text{mid}}=\lambda_0/(2n_{\text{mid}})=\lambda/2$. Different thicknesses for the DBR constituent layers, or for the middle region, or both, will shift the design wavelength. For middle layer thicknesses greater than λ, two or more resonance wavelengths will exist within the high reflectivity region of the DBR mirrors.

The reflection spectrum of a reference wafer is shown in Fig. 2. A high reflectivity region extends from 1000 to 1800 nm, with a reflection dip at the cavity resonance of 1350 nm. The reflection dip drops to 10% and has a width of 10 nm (7 meV). By fine tuning the top mirror reflectivity, the reflection on resonance can theoretically be reduced to zero. The spectral width of the reflectance dip $\Delta\lambda_0$ at wavelength position λ_0 is given by[1]

$$\frac{\Delta\lambda_0}{\lambda_0}=\frac{\lambda}{2L_{\text{Cav}}}\left(\frac{1-\sqrt{R_1R_2}}{\pi^4\sqrt{R_1R_2}}\right). \tag{2}$$

 © 1993 American Institute of Physics

Downloaded 30 Jun 2003 to 128.113.111.105. Redistribution subject to AIP license or copyright, see http://ojps.aip.org/aplo/aplcr.jsp

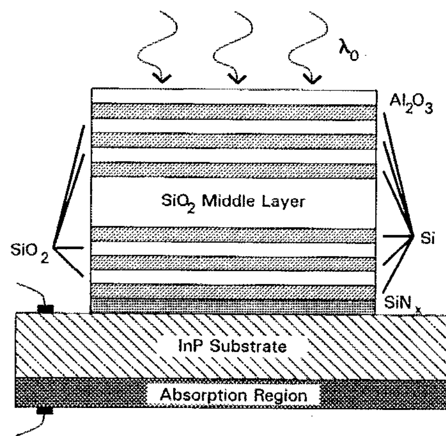

FIG. 1. The structure of a Fabry–Perot resonant microcavity evaporated on the light collecting surface of a standard *p-i-n* photodetector. Two equal reflectivity DBR mirrors surround a middle SiO_2 layer. The resulting device is a wavelength selective detector.

The top and bottom mirror reflectivities are R_1 and R_2, respectively. The effective cavity length L_{Cav} is a multiple of the wavelength of light λ within the cavity. For our structures $L_{Cav} \approx 0.9\lambda$ resulting from a 0.5λ central SiO_2 region and a 0.2λ effective penetration depth into each DBR mirror. This L_{Cav} is much shorter than the values obtainable in a semiconductor RCE detector, which are typically greater than 2.5λ because of much greater mirror penetration depth. The smaller L_{Cav} and large spectrum of high reflectance in our device is due to the large index difference between the Si layers in the DBR ($n \approx 3.5$) and the SiO_2 layers ($n \approx 1.46$). The theoretical mirror reflectivities are about 0.96, which gives a theoretical width of about 11 nm, which is close to what is observed. Because we are free to chose from a large variety of materials for the mirror layers, with a wide range of refractive indices, the spectral width and reflectance width can be tailored independently of the total mirror reflectivity.

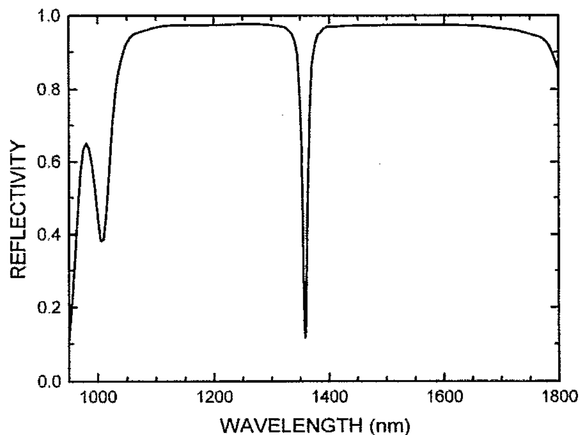

FIG. 2. The reflection spectrum of a test wafer with a Fabry–Perot microcavity grown at the same time as the one on the photodetector. A reflectance dip 11.5 nm wide is seen at 1350 nm corresponding to the transmission resonance of the microcavity.

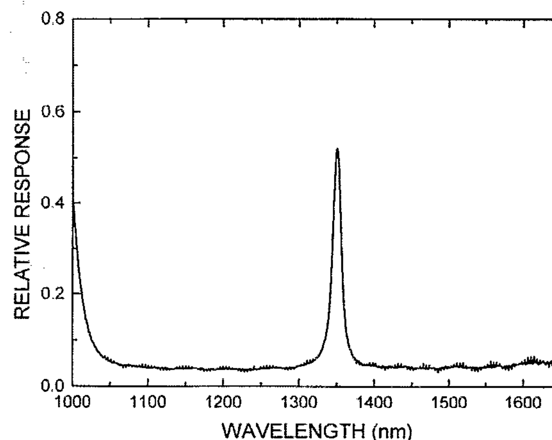

FIG. 3. The detected photocurrent from a RC-*PIN* detector with a deposited Fabry–Perot cavity, divided by the photocurrent from a reference detector with an antireflection coating but no cavity. The detection is low from 1100 to 1800 nm except for the 14 nm wide resonance at 1350 nm where the relative detection is 52%.

A lossless microcavity filter transmits 100% of the light on resonance if the top and bottom DBR mirrors are of equal reflectivities, or $R_1 = R_2$. Similar mirror reflectivity constraints are also seen in RCE detectors.[2] For a RCE photodetector, with an active medium with single-pass transmission T (including any antinode effects), the detection efficiency is a maximum only when $R_1 = R_2 T^2$, with a value of 100% only if $R_2 = 1$. The equal mirror reflectivity constraint of our microcavity is certainly easier to realize than the dual constraints needed in a RCE detector. In both types of optimized devices, the maximum theoretical contrast ratio between on-resonance detection, and off-resonance detection is given by $(1+R_1^2)/(1-R_1)^2$.

The response of a detector with cavity versus wavelength, relative to a detector with antireflective coating, is given in Fig. 3. The figure illustrates that light is detected only at the resonance wavelength of 1350 nm, whereas the detector is insensitive to all other wavelengths from 1100 to 1700 nm. The reflected light can, in principle, be detected by other RC-*PIN*s, constituting a wavelength-division multiplexing system. The maximum relative responsivity at 1350 nm wavelength is 52%, while the response off resonance is about 4%. The discrepancy between the 10% reflection and the 52% response can theoretically be explained by an absorption coefficient of 150 cm^{-1} in the amorphous silicon. Growth at higher temperatures, or by CVD deposition can produce silicon layers with reduced absorption, and therefore greater detection efficiency. Other high index materials, such as TiO_2, can be substituted with no absorption loss, but with less wavelength range of suppression. Other possible sources of efficiency loss are light scattering in the films, or a slightly bumpy substrate surface resulting in a smearing of the microcavity transmission peak. The off-resonance response of 4% is higher than the calculated 0.1% for a perfect layer structure with mirror reflectivities of 96%. This can be due to scattered light, either from the surrounding detector mount, or within the layers themselves, or from the far side

Downloaded 30 Jun 2003 to 128.113.111.105. Redistribution subject to AIP license or copyright, see http://ojps.aip.org/aplo/aplcr.jsp

of the detector. Any reflections from the far side of detector, whether specular of diffuse, will reduce the detected signal on resonance, and increase it off resonance.

The resonance wavelength is relatively insensitive to small deviations of incidence angle from the normal, but shifts quickly at higher angles. The resonance wavelength versus incidence angle θ_0 is given by[6]

$$\lambda_{\rm res}(\theta_0)=\lambda_{r0}\cos\{\sin^{-1}[\sin(\theta_0)/n_c]\}. \quad (3)$$

The value n_c is an effective index of refraction for the microcavity, which can be determined by fitting this formula to measured or calculated shifts with angle. For our devices $n_c \approx 1.75$. The range of angles of a monochromatic incoming light beam should be restricted such all of the rays are within the resonance peak. Devices with thin resonance peaks or with low n_c therefore require more collimated input beams for maximum detection efficiency. For our structure, the resonance width is 14 nm at a wavelength of 1350 nm. The maximum coupling efficiencies for ideal-wavelength monochromatic light transmitted through (or detected by) a cavity with effective index n_c, from a light cone of numerical aperature $N_A=\sin(\theta_{0,\max})$, for various fractional linewidths $t=\Delta\lambda_0/\lambda_0$ is given by the following formula:

$$\text{Maximum efficiency}(N_A/n_c) = \left[\tan^{-1}\left(\frac{1-\cos[\sin^{-1}(N_A/n_c)]}{t}\right)\right] \Big/ \times\left(\frac{1-\cos[\sin^{-1}(N_A/n_c)]}{t}\right). \quad (4)$$

The calculation assumes a uniform intensity of light over all solid angles within the light cone, and includes only the effect of resonance shift with angle, assuming no change in the peak detection efficiency with angle. A graph of efficiency relative to a parallel beam for various fractional linewidths is given in Fig. 4. One can see that for our device with $t=0.01$, and $n_c=1.75$, the relative coupling efficiency for a light cone with $N_A<0.29$ is greater than 0.69, and for $N_A<0.20$ is greater than 0.89.

An incident beam with rays experiencing resonance wavelength shifts up to the value of the resonance width results in relative efficiency of 78.5%. For larger *NA* values, the relative efficiency drops rapidly. A microcavity should therefore be designed to have a relative efficiency larger than 78.5% for the given *NA* of the light source. Our cavity meets this criterion for numerical aperature values less than 0.25. Larger *NA* values can be achieved by designing a slightly wider spectral width, or a similar spectral width and a larger n_c. The cavity index n_c can be increased by replacing the central SiO_2 region, or even all SiO_2 layers, by a higher index material.

We have demonstrated a resonant-cavity *p-i-n* photodetector based on the reflection or transmission through a

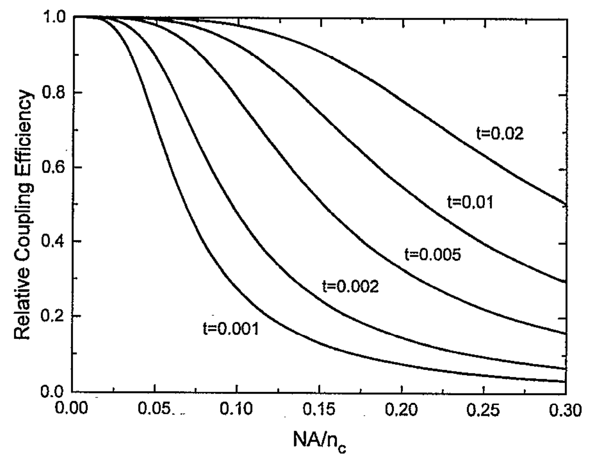

FIG. 4. The maximum relative response of our Fabry–Perot cavity for various fractional resonance widths t vs N_A/n_c: the numerical aperature of the incoming light divided by the effective refractive index of the cavity. The detector response for a collimated beam exactly at the resonance wavelength at some particular input angle is defined as unity. These curves may also be used RCE detectors.

Si/SiO_2 Fabry–Perot cavity electron-beam deposited on the InP substrate of a commercial InGaAs photodetector. The detection efficiency relative to a reference device was 52% at the resonant wavelength of 1350 nm, with a resonance width of 14 nm, and a 4% response for off-resonance wavelengths in the 1100–1700 nm range. We show that the new detector has several clear advantages over the RCE photodetector. Our RC-*PIN* detector incorporates nonepitaxial, amorphous electron-beam deposited layers on the light-gathering side of a conventional *p-i-n* detector. Because of the large index difference of component layers, as well as the large range of material indices to chose from (from $n=1.26$ for CaF_2 to $n=3.5$ for Si), our RC-*PIN* structure has highly tailorable spectral position, spectral detection width, spectral reflection width, and maximum numerical aperature of efficient detection. The microcavity of our RC-*PIN* design can also be deposited on an existing detector structure, without modification of semiconductor growth. Such a photodetector would be useful for wavelength demultiplexing applications.

The authors would like to thank J. C. Bean and L. Marchut for contributions to this work.

[1] N. E. J. Hunt, E. F. Schubert, R. A. Logan, and G. J. Zydzik, Appl. Phys. Lett. **61**, 2287 (1992).
[2] A. Chin and T. Y. Chang, J. Vac. Sci. Technol. B **8**, 339 (1990).
[3] K. Kishino, M. S. Ünlü, J.-I. Chyi, J. Reed, L. Arsenault, and H. Morkoç, IEEE J. Quantum Electron. **27**, 2025 (1991).
[4] A. G. Dentai, R. Kuchibhotla, J. C. Campbell, C. Tsai, and C. Lei, Electron. Lett. **27**, 2125 (1991).
[5] U. Prank, M. Mikulla, and W. Kowalsky, Appl. Phys. Lett. **62**, 129 (1993).
[6] E. F. Schubert, A. M. Vredenberg, N. E. J. Hunt, Y. H. Wong, P. C. Becker, J. M. Poate, D. C. Jacobson, L. C. Feldman, and G. J. Zydzik, Appl. Phys. Lett. **61**, 1381 (1992).

Downloaded 30 Jun 2003 to 128.113.111.105. Redistribution subject to AIP license or copyright, see http://ojps.aip.org/aplo/aplcr.jsp